Available online at www.sciencedirect.com

ScienceDirect

Ceramics International 37 (2011) 1245–1249

CERAMICS
INTERNATIONAL

www.elsevier.com/locate/ceramint

Analysis of structural and thermal properties of Li_2TiO_3 ceramic powders

R. Ramaraghavulu [a], S. Buddhudu [a,*], G. Bhaskar Kumar [b]

[a] *Department of Physics, Sri Venkateswara University, Tirupati 517502, India*
[b] *Alternative Energy and Nanotechnology Laboratory, Department of Physics, Indian institute of Technology, Chennai 600036, India*

Received 6 August 2010; received in revised form 28 October 2010; accepted 1 December 2010
Available online 21 January 2011

Abstract

Li_2TiO_3 ceramic powders have been developed by a solid state reaction method and those have been sintered at four different temperatures (600 °C, 700 °C, 800 °C and 900 °C) towards the optimization of sintering temperature that has been found to be at 800 °C based on the nature of the XRD profiles. The sample sintered at 800 °C has shown a good crystallinity situation from its XRD peaks and the sample is found to be in monoclinic structure which is in accordance with the reported data of JCPDS 33-0831. The SEM images for samples sintered at 600 °C, 700 °C, 800 and 900 °C, EDAX peaks, FTIR profile have been measured for the temperature optimized (800 °C) sample for understanding the structural details of Li_2TiO_3 ceramic powders. Besides these, dielectric constant, dielectric loss and a.c. conductivities have been measured for the temperature optimized sample. In order to strengthen the observations made in the XRD profiles at four different temperatures, Raman spectra of those four sintered ceramic powders have also been studied. In respect of the thermal properties, only for the as synthesized (precursor) sample, simultaneous measurement of TG-DTA profiles has been carried out for analysis.

Keyword : Ceramic powder-characterization

1. Introduction

Morphology and important applications of Li_2TiO_3 ceramics have earlier been reported in literature [1–6]. Keeping the uniqueness and relevance of this material, we have considered this host matrix to incorporate with Eu^{3+} and Dy^{3+} ions separately for their potential applications in the development of visible luminescent colors [7]. While studying luminescent properties of Eu^{3+}:Li_2TiO_3 and Dy^{3+}:Li_2TiO_3 ceramics, we have not earlier undertaken to study structural, thermal, Raman and dielectric properties for the host matrix Li_2TiO_3 ceramic powder, as our major objective was on luminescent performances. In the present work structural, thermal and dielectric studies have been taken up and the interesting results are reported here.

2. Experimental studies

Lithium titanium oxide (Li_2TiO_3) ceramic powder was synthesized by a solid state reaction method based on the following reaction scheme:

$$Li_2CO_3 + TiO_2 \rightarrow Li_2TiO_3 + CO_2$$

Li_2TiO_3 ceramic powder was prepared by mixing the chemicals appropriately in an agate motor using the acetone as the binder solvent for 2 h to obtain homogeneous mixture and then that was collected into porcelain crucibles for sintering each of those samples at 600 °C, 700 °C, 800 °C and 900 °C for 5 h, respectively.

The prepared powder ceramics were characterized by XRD 3003 Seifert diffractometer with Cu K_α line of $\lambda = 1.5406$ Å. The data were collected in the 2θ range from 15° to 70° at the rate of 0.05°/s. The crystallite size was calculated by using full width at half maxima (FWHM) by using Scherrer's equation $D_{\text{crystallite}} = k\lambda/\beta \cos\theta$. Where D was the crystallite size, k was Scherrer's constant = 0.9, λ =1.5406 Å (X-ray wavelength), and β was full width half maxima at diffraction angle 2θ. Thermal analysis of as prepared sample studied, differential thermal analysis (DTA) and thermogravimetric analysis (TGA) were measured for the precursor (as synthesized sample) in N_2 atmosphere at a heating rate of 10 °C/min on a Netzesch STA 409 simultaneous thermal analyzer. Raman spectrum was recorded using a Horiva Jobin HR800 spectrometer. The

---

* Corresponding author.
E-mail address: profsb_svuniv@hotmail.com (S. Buddhudu).

0272-8842/$36.00 © 2011 Elsevier Ltd and Techna Group S.r.l. All rights reserved.
doi:10.1016/j.ceramint.2010.12.007

samples were excited with a 632.8 nm of He–Ne laser and the profile was obtained in the range of 100–1000 cm^{-1} with spectral resolution of 1 cm^{-1}. The morphology of the ceramic powder was examined on a JEOL JSEM 840A scanning electron microscope. The elemental analysis of the synthesized product was carried out using the EDAX attachment to the SEM system. A Fourier transform infrared (FTIR) spectrum of the sample was carried out on a Thermo Nicolet-5700 spectrophotometer using the KBr pellet technique in the range of 4000–400 cm^{-1}.

Dielectric properties were performed using Agilent 4294A precision LCR meter. For measuring the dielectric constant, pressed cylindrical pellets of Li_2TiO_3 sintered at 800 °C was covered on surfaces with silver paste, there by forming parallel plate capacitor geometry. The dielectric measurements were carried out from 5 kHz to10 MHz. The value of the dielectric constant (ε') of Li_2TiO_3 was calculated using the formula:

$$\varepsilon' = \frac{Cd}{\varepsilon_0 A}$$

where ε_o is permittivity in vacuum equal to 0.0885 pF/cm^2, C is the capacitance of the specimen, t is the sample thickness and A is the area of the specimen in cm^2.

The a.c. conductivity of Li_2TiO_3 that was calculated from the relation:

$$\sigma_{\text{a.c.}} = \varepsilon' \varepsilon_0 \omega \tan\delta (\text{Ohm}^{-1} \times \text{cm}^{-1})$$

where ε_o is the permittivity in vacuum and ω is $2\pi f$ and tan δ is loss tangent which is proportional to the loss of energy from the applied field on the sample and therefore donated as dielectric loss.

3. Results and discussion

The XRD patterns of the Li_2TiO_3 powders, sintered at different temperatures are shown in Fig. 1 and features have demonstrated the monoclinic phase from the ceramic powder that was calcined at 800 °C, and found to be well matching with JCPDC 33-0831 with $a = 5.069$, $b = 8.799$, $c = 9.759$, $\beta = 100.2$. XRD diffractogram of Li_2TiO_3 powder at 600 °C has shown small intense peaks at $2\theta = 27.54°$, and 54.55° which correspond to the rutile TiO_2 [8,9]. Three other peaks located at $2\theta = 21.35°$, 30.53° and 31.69° correspond to the impurity of the precursor. XRD difractogram of Li_2TiO_3 that was calcined at 700 °C has not shown such a rutile TiO_2 peaks and hence found to be commencing to transform into the monoclinic Li_2TiO_3 phase. With an increase in calcination temperature, the peaks are becoming sharp and intense due to an increase in crystallite size of the sample. The crystallite size was calculated by using Scherrer's equation, which results in with an average crystallite size 19, 26, 30 and 42 nm corresponding to the Li_2TiO_3 powders that were sintered at 600 °C, 700 °C, 800 °C and 900 °C. Variation of crystallite size with the calcination temperature change is given in Fig. 2.

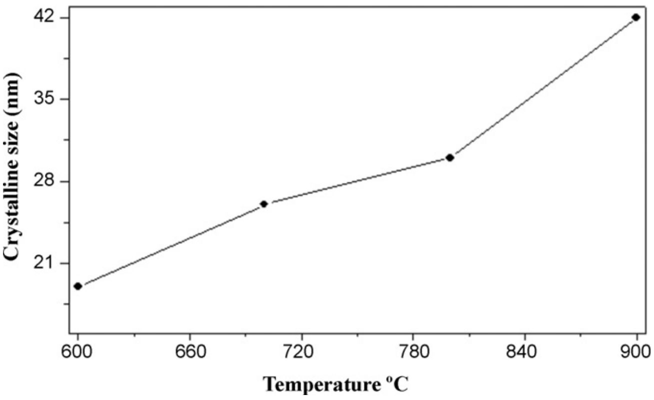

Fig. 2. Variation of crystallite size with change in sintering temperature.

Fig. 3 shows the TG-DTA curves of the as synthesized (precursor) sample of Li_2TiO_3. It can be clearly seen from this figure that the formation of the Li_2TiO_3 takes places around 728 °C. It can be observed that there are two stages in mass losses of the material and then it becomes constant from 728 °C up to 1000 °C. The major weight loss 25.62% occurs in the single step between 500 and 728 °C. Before reaching to 500 °C, the total weight loss is 3.45%. The mass loss from room temperature to 728 °C could be due to the evaporation of water

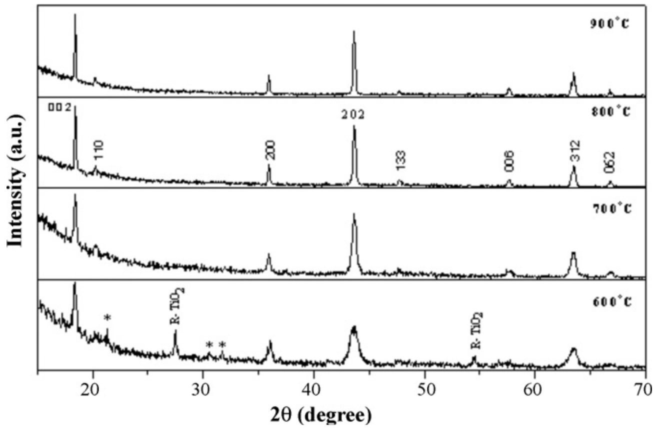

Fig. 1. XRD profiles of Li_2TiO_3 ceramic powders sintered at 600 °C, 700 °C, 800 °C and 900 °C for 5 h.

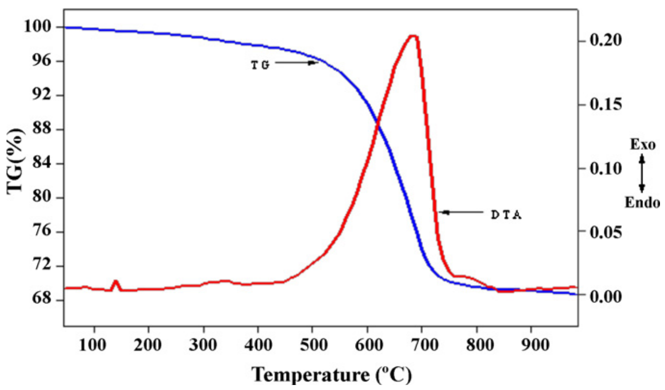

Fig. 3. TG-DTA profiles of as synthesized Li_2TiO_3 ceramic powder.

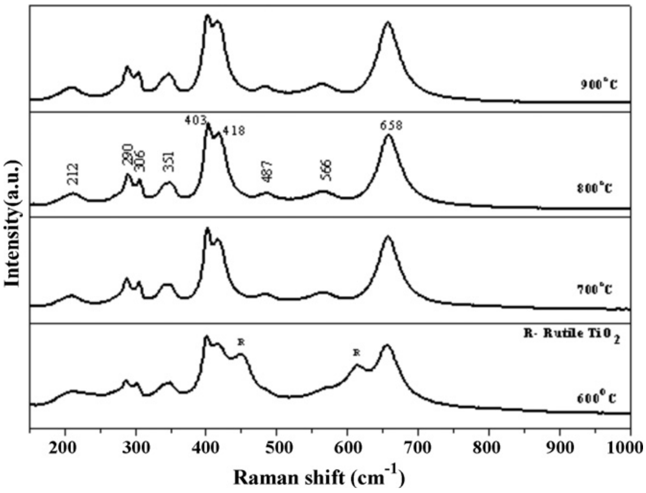

Fig. 4. Raman spectra of Li_2TiO_3 ceramic powders at 600 °C, 700 °C, 800 °C and 900 °C for 5 h.

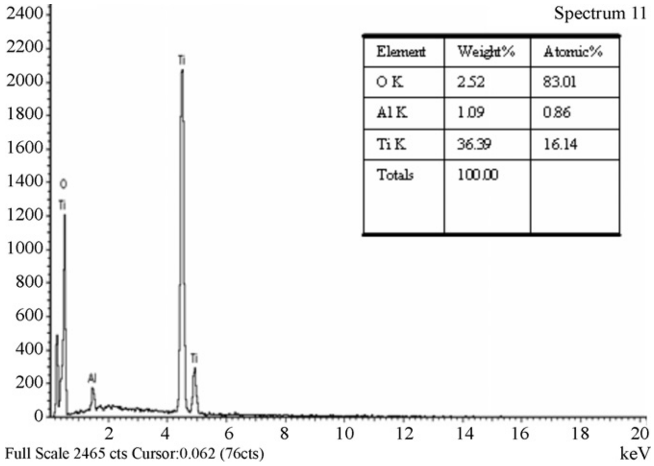

Element	Weight%	Atomic%
O K	2.52	83.01
Al K	1.09	0.86
Ti K	36.39	16.14
Totals	100.00	

Fig. 6. EDAX analysis of Li_2TiO_3 powder sintered at 800 °C for 5 h.

and decomposition of thermally unstable organic compounds if any. We get the weight of Li_2TiO_3 at 728 °C is 70.93% it is well matched with calculated value 71.40%. This result gives the TG curve of as prepared Li_2TiO_3. A broad exothermic peak appeared near 685 °C in the DTA curve reveals the crystallization of Li_2TiO_3 ceramic powder.

Raman spectra of Li_2TiO_3 ceramic powder at 600 °C, 700 °C, 800 °C and 900 °C as shown in Fig. 4. Raman spectrum at the calcination temperature of 600 °C displays two intense peaks at 451 cm^{-1} and 615 cm^{-1}, which correspond to the rutile TiO_2 [10,11]. The calcination temperature of 60–600 °C has been reported in the case of the appearance of TiO_2 (rutile) phase [12,13]. These rutile peaks disappear in Raman spectrum at 700 °C. In lithium titanate, the frequencies in the 700–550 cm^{-1} region are known to be assigned to Ti–O stretching in TiO_6 octahedra. In oxides, where lithium is octahedrally coordinated by oxygen; the frequencies of Li–O stretching are known to be existing within the 250–400 cm^{-1} region. In the lithium coordination is tetragonal; the frequencies lie in the 400–550 cm^{-1} region. In the Li_2TiO_3 structure, the lithium occupies both the octahedral and tetrahedral positions [13,14].

Fig. 5 shows the SEM micrographs of the Li_2TiO_3 ceramic powders which are sintered at 600 °C, 700 °C, 800 °C and 900 °C each for 5 h for a comparison purpose. From these

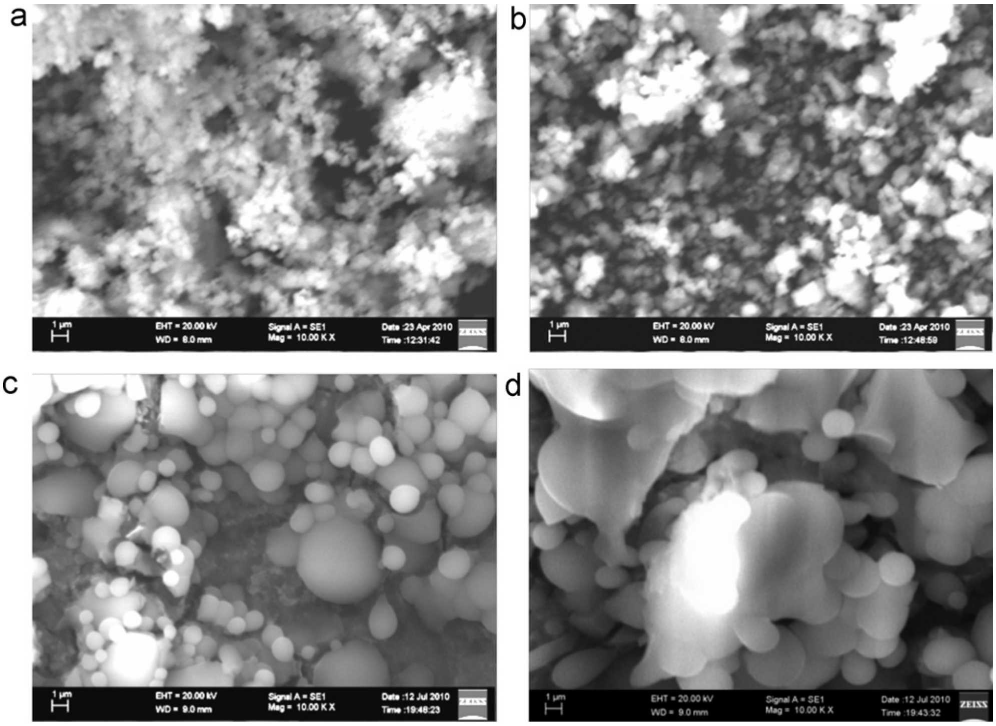

Fig. 5. SEM micrographs showing Li_2TiO_3 powders sintered at (a) 600 °C and (b) 700 °C, (c) 800 °C and (d) 900 °C each for 5 h.

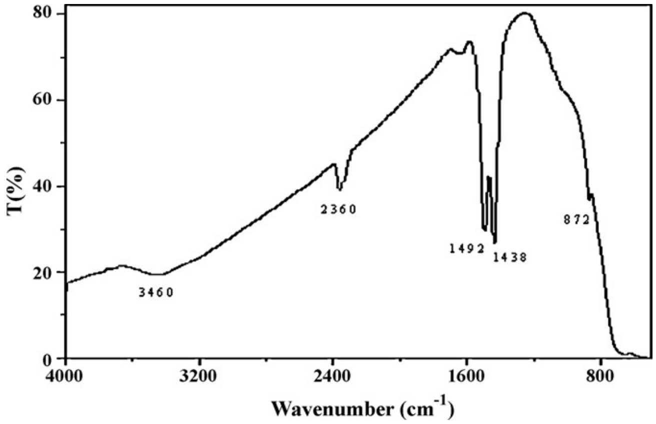

Fig. 7. FT-IR spectrum of Li_2TiO_3 powders sintered at 800 °C for 5 h.

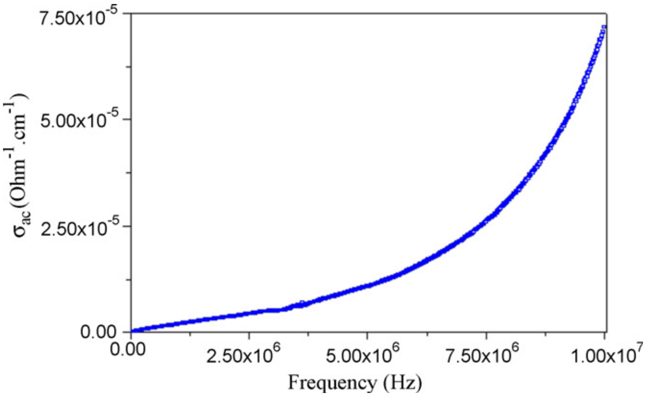

Fig. 9. Variation of a.c. conductivity with frequency for Li_2TiO_3 sintered at 800 °C for 5 h.

images it is clear to notice that the sample sintered at 800 °C has revealed clearer and well defined structures with granular size in about 1 μm. Fig. 6 presents the EDAX elemental analysis of the ceramic powder studied. However, the EDAX of the matrix could not show the presence of lithium because of its light weight [15,16]. The impurity of Al was found to be in (0.86%) from the EDAX analysis of Li_2TiO_3 shows this Al impurity which could be arising due to the Li_2TiO_3 or TiO_2.

The FT-IR spectrum of Li_2TiO_3 is shown in Fig. 7 with a broad peak at 3460 cm^{-1} that arises due to the O–H stretching vibrations of free and hydrogen-bonded surface hydroxyl groups [17]. The bonds at 1498 cm^{-1} and 1433 cm^{-1} can be assigned to the antisymmetric stretching vibrations of CO_3^{2-} anions and that a peak located at 872 cm^{-1} can be attributed to the stretching vibrations of CO_3^{2-} anions [18]. The bond at 2360 cm^{-1} is due to the Ti–O vibrations [18]. Another peak located at 2360 cm^{-1} is due to the Ti–O vibrations [19].

Fig. 8 shows the frequency dependence of the dielectric constant and dielectric loss of Li_2TiO_3 ceramic powder that was sintered at 800 °C measured in the frequency range from 5 kHz to 10 MHz at the room temperature. In Fig. 8, it is seen that the dielectric constant and dielectric loss decreases up to 1 MHz indicating the fact that the carriers do not follow alternating field up to this frequency. Beyond this frequency (1–10 MHz) the dielectric constant and dielectric loss has been found to be increasing with an increase in the frequency. The a.c. conductivity has been shown in Fig. 9 evaluated from the data of dielectric measurements also found to be changing with an increase in the frequency. The reason behind this phenomenon may be that during the synthesis process, some vacancies might be possible in the system. Such vacancies may change the oxidation state of Ti ions (Ti^{4+} to Ti^{3+}), which in turn increase the number of electrons. Such a mechanism could increase the hopping process and thus causing an increase in the dielectric constant, tan δ, and a.c. conductivity [20–22].

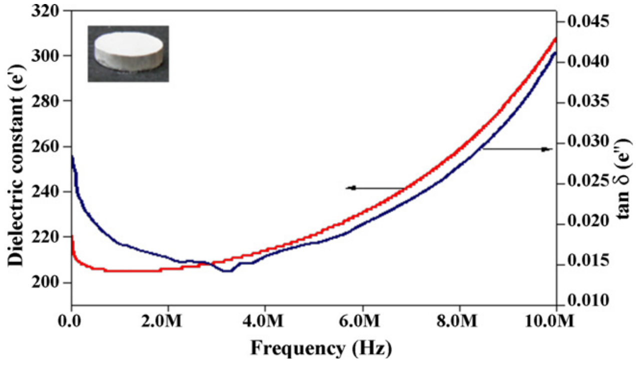

Fig. 8. Dielectric constant and dielectric loss of Li_2TiO_3 pellets sintered at 800 °C for 5 h (inset figure shows the pellet form of Li_2TiO_3 ceramic powder).

4. Conclusion

Li_2TiO_3 ceramic powders were developed by a solid state reaction method at four different temperatures such as 600 °C, 700 °C, 800 °C and 900 °C and the sample sintered at 800 °C was exhibiting satisfactory structural properties. Therefore, the optimized sintering temperature was found to be at 800 °C based on XRD profiles and SEM micrographs. In order to understand the thermal properties, precursor Li_2TiO_3 was considered to measure its TG-DTA profile. For this optimized sample, both, Raman spectra and dielectric properties have also been studied.

References

[1] S.J. Lee, Characteristics of lithium titanate fabricated by an organic–inorganic solution route, J. Ceram. Proc. Res. 9 (1) (2008) 64–67.

[2] Th. Fehr a, E. Schmidbauer b, Electrical conductivity of Li_2TiO_3 ceramics, Solid State Ionics 178 (2007) 35–41.

[3] C.-H. Jung, J.-Y. Park, W.-J. Kim, W.-S. Ryu, S.-J. Lee, Characterizations of Li_2TiO_3 prepared by a solution combustion synthesis and fabrication of spherical particles by dry-rolling granulation process, Fusion Eng. Des. 81 (2006) 1039–1044.

[4] G. Vitins, G. Kizane, A. Lusis, G. Kizane, A. Lusis, J. Tiliks, Electrical conductiviy studies in the system Li_2TiO_3–$Li_{1.33}Ti_{1.67}O_4$, J. Solid State Electrochem. 6 (2006) 311–319.

[5] K. Kataoka, Y. Takahashi, N. Kijima, H. Nagai, J. Akimoto, Y. Idemoto, K.-I. Ohshima, Crystal growth and structure refinement of monoclinic Li_2TiO_3, Mater. Res. Bull. 44 (2009) 168–172.

[6] A. Sinha, S.R. Nair, P.K. Sinha, Single step synthesis of Li_2TiO_3 powder, J. Nucl. Mater. 399 (2010) 162–166.

[7] G. Bhaskar Kumar, S. Buddhudu, Synthesis and emission analysis of RE^{3+} (Eu^{3+} or Dy^{3+}):Li_2TiO_3 ceramics, Ceram. Int. 35 (2009) 521–525.

[8] E. Haro-Poniatowski, T. Lopez, E. Torres, L. Escobar-AlarcóN, M. Picquart, Structural study of lithium titanium mixed oxides prepared by sol–gel process, J. Mater. Sci. 37 (2002) 3241–3249.

[9] J. Garcia-Serrano, E. Gomez-Hernandez, M. Ocamp-Fernandez, U. Pal, Effect of Ag doping on the crystallization and phase transition of TiO_2 nonoparticles, Curr. Appl. Phys. 9 (2009) 1097–1105.

[10] M.G. Navarro-Rojero, J.J. Romero, F. Rubio-Marcos, J.F. Fernandez, Intermediate phases formation during the synthesis of $Bi_4Ti_3O_{12}$ by solid state reaction, Ceram. Int. 36 (2010) 1319–1325.

[11] X. Wu, M.-S. Zhang, Z. Yin, X. Ji, Q. Chen, Temperature characteristics of Raman spectra in nanometer material titanium dioxide, Chin. Phys. Lett. 11 (11) (1994) 685.

[12] D. Yamaki, T. Nakazawa, T. Tanifuji, T. Aruga, S. Jitsukawa, K. Hojou, Observation of the microstructural changes in lithium titanate by multi-ion irradiation, J. Nucl. Mater. 329–333 (2004) 1279–1282.

[13] T. Nakazawa, A. Naito, T. Aruga, V. Grismanovs, Y. Chimi, A. Iwase, S. Jitsukawa, High energy heavy ion induced structural disorder in Li_2TiO_3, J. Nucl. Mater. 367–370 (2007) 1398–1403.

[14] T. Nakazawa, V. Grismanovs, D. Yamaki, Y. Katano, T. Aruga, Disordering in Li_2TiO_3 irradiated with high energy ions, Nucl. Instrum. Methods Phys. Res., Sect. B 206 (2003) 166–170.

[15] A. Fini, G. Fazio, M.A. Holgado, M.J.F. Herva, Fractal and reactive dimensions of some ursodeoxycholic acid salts, Int. J. Pharm. 171 (1998) 45–52.

[16] Y. Kojima, K. Suzuki, Y. Kawai, Hydrogen generation from lithium borohydride solution over nano-sized platinum dispersed on $LiCoO_2$, J. Power Sources 155 (2006) 325–328.

[17] X. Liu, P. Jia, J. Lin, G. Li, Monodisperse spherical core–shell structured SiO_2–$CaTiO_3$:Pr^{3+} phosphors for field emission displays, J. Appl. Phys. 99 (2006) 124902.

[18] D.R. Zhang, H.L. Liu, R.H. Jin, N.Z. Zhang, Y.X. Liu, Y.S. Kang, Synthesis and characterization of nanocrystalline $LiTiO_2$ using a one-step hydrothermal method, J. Ind. Eng. Chem. 13 (2007) 92–96.

[19] Y. Li, H. Zhao, Z. Tian, W. Qiu, X. Li, Solvothermal synthesis and electrochemical characterization of amorphous lithium titanate materials, J. Alloys Compd. 455 (1–2) (2008) 471–474.

[20] J. Maxwell, James Clerk, A Treatise on Electricity and Magnetism, vol. 1, Section 328, Oxford Press, London, 1873.

[21] C.G. Koops, On the dispersion of resistivity and dielectric constant of some semiconductors at audiofrequencies, Phys. Rev. 83 (1951) 121.

[22] S. Kumar, R. Kumar, B.H. Koo, H. Choi, D.U. Kim, C.G. Lee, Structural and electrical properties of Mg_2TiO_4, J. Ceram. Soc. Jpn. 117 (5) (2009) 689–692.